Published in final edited form as:

ACS Chem Biol. 2024 June 21; 19(6): 1291–1302. doi:10.1021/acschembio.4c00100.

Endogenous Cellular Metabolite Methylglyoxal Induces DNA–Protein Cross-Links in Living Cells

Alexander K. Hurben,

Department of Medicinal Chemistry, University of Minnesota, Minneapolis, Minnesota 55455, United States; Present Address: Department of Chemistry, University of California, Berkeley, California 94720, United States

Qi Zhang,

Department of Medicinal Chemistry, University of Minnesota, Minneapolis, Minnesota 55455, United States

James J. Galligan,

Department of Pharmacology and Toxicology, College of Pharmacy, University of Arizona, Tucson, Arizona 85721, United States

Natalia Tretyakova*,

Department of Medicinal Chemistry, University of Minnesota, Minneapolis, Minnesota 55455, United States; Masonic Cancer Center, University of Minnesota, Minneapolis, Minnesota 55455, United States

Luke Erber*

Department of Medicinal Chemistry, University of Minnesota, Minneapolis, Minnesota 55455, United States

Abstract

Methylglyoxal (MGO) is an electrophilic α-oxoaldehyde generated endogenously through metabolism of carbohydrates and exogenously due to autoxidation of sugars, degradation of lipids, and fermentation during food and drink processing. MGO can react with nucleophilic sites within proteins and DNA to form covalent adducts. MGO-induced advanced glycation

***Corresponding Authors Natalia Tretyakova** – *Department of Medicinal Chemistry, University of Minnesota, Minneapolis, Minnesota 55455, United States; Masonic Cancer Center, University of Minnesota, Minneapolis, Minnesota 55455, United States;* trety001@umn.edu, **Luke Erber –** *Department of Medicinal Chemistry, University of Minnesota, Minneapolis, Minnesota 55455, United States;* Present Address: Department of Medicinal Chemistry, University of Kansas, Lawrence, Kansas 66044, United States; erber@ku.edu.

Author Contributions

L.E., A.K.H., and N.T. conceptualized and designed this study. Experimentally, A.K.H. performed synthesis, conducted cell culture, and generated in vitro DPCs. Q.Z. performed radiolabeled DPC assays. J.J.G. provided GLO1 KO cells and aided in developing cell culture experiments. L.E. performed DPC isolation and characterization by mass spectrometry-based proteomics. The manuscript was written and approved by all authors

The authors declare no competing financial interest.

ASSOCIATED CONTENT

Supporting Information

The Supporting Information is available free of charge at https://pubs.acs.org/doi/10.1021/acschembio.4c00100.

Supporting results (Figures S1–S19); proteomics results (Tables S1–S3), materials and methods, synthetic procedures for generating analytical standards, and NMR spectra characterizing synthetic products (PDF)

Complete contact information is available at: https://pubs.acs.org/10.1021/acschembio.4c00100

end-products such as protein and DNA adducts are thought to be involved in oxidative stress, inflammation, diabetes, cancer, renal failure, and neurodegenerative diseases. Additionally, MGO has been hypothesized to form toxic DNA–protein cross-links (DPC), but the identities of proteins participating in such cross-linking in cells have not been determined. In the present work, we quantified DPC formation in human cells exposed to MGO and identified proteins trapped on DNA upon MGO exposure using mass spectrometry-based proteomics. A total of 265 proteins were found to participate in MGO-derived DPC formation including gene products engaged in telomere organization, nucleosome assembly, and gene expression. *In vitro* experiments confirmed DPC formation between DNA and glyceraldehyde-3-phosphate dehydrogenase (GAPDH), as well as histone proteins H3.1 and H4. Collectively, our study provides the first evidence for MGO-mediated DNA–protein cross-linking in living cells, prompting future studies regarding the relevance of these toxic lesions in cancer, diabetes, and other diseases linked to elevated MGO levels.

Graphical Abstract

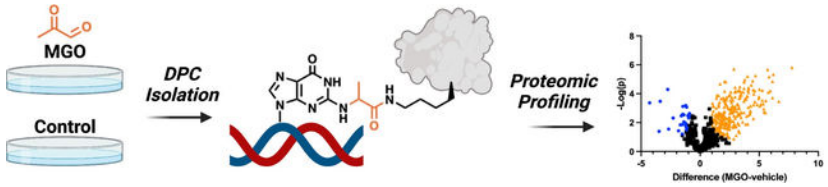

INTRODUCTION

DNA–protein cross-links (DPCs) are toxic lesions that form upon covalent trapping of cellular proteins to DNA. DPCs can be induced by exposure to various physical and chemical agents including endogenous metabolites such as formaldehyde,[1] reactive oxygen species,[2,3] exogenous chemicals such as [1,3]-butadiene,[4–6] ionizing radiation,[7] UV light,8 and transition metals,[9] as well as chemotherapeutic agents including platinum drugs,[10] nitrogen mustards,[11–13] and haloethylnitrosoureas.[14] Bulky DNA–protein lesions distort the DNA helix, thereby obstructing essential DNA–protein interactions necessary for DNA replication, transcription, repair, recombination, and chromatin remodeling.[8,15–17] If not repaired, DPCs lead to permanent DNA alterations and toxicity.[8,18–20] Endogenous DPC levels are elevated in individuals suffering from Ruijs–Aalfs syndrome, a genetic disorder defined by polymorphisms in the SPRTN gene which encodes a protease involved in DPC repair. Patients with Ruijs–Aalfs syndrome exhibit genomic instability, premature aging, and develop hepatocellular carcinoma.[21–23]

Despite ubiquitous formation of DPCs in cells and their possible implications in human disease, the structural identities and repair pathways for this class of adducts are not completely understood due to their chemical heterogeneity and challenges in studying bulky biomolecular conjugates containing characteristics of proteins and DNA. Mass spectrometry-based studies have identified hundreds of proteins that participate in cross-linking to nuclear DNA upon exposure to electrophilic endogenous metabolites, exogenous chemicals, and therapeutic agents.[6,12,24] This cross-linking occurs on nucleophilic side chains of amino acids of known DNA binding partners such as repair proteins, histones,

and transcription factors, as well as with gene products that have no documented DNA affinity.[20] Cross-linking targets multiple sites of DNA, including the C-5 methyl group of thymine, the N7 of guanine, and exocyclic amines of adenine, cytosine, and guanine.[19] If not repaired, DPCs constitute a complete block to replication and transcription machinery and thus represent a serious threat to cell viability.[15,25–27] With the exception of topoisomerase DPCs that can be directly reversed by tyrosyl-DNA phosphodiesterases (TDP1 and TDP2),[28] cellular repair of DPCs requires the activity of proteolytic enzymes to break the protein down to smaller peptides.[15,29–31] The resulting DNA–peptide cross-links (DpC) can be bypassed by DNA polymerases[26,32–34] and are subject to canonical DNA repair pathways.[35–37] Proteolytic cleavage can be accomplished through the activity of SPRTN metalloprotease[38] or the proteasome.[39] DNA repair pathways participating in DpC tolerance and repair include translesion synthesis polymerases[27,32] and the nucleotide excision pathway (NER).[40,41]

Methylglyoxal (MGO) is an electrophilic α-oxoaldehyde byproduct of cellular metabolism capable of reacting with nucleophilic biomolecules to form a diverse set of covalent adducts.[42] In living cells, MGO is primarily derived through the spontaneous degradation of the triose phosphate intermediates of glycolysis and is present at low micromolar (1–10 μM) concentrations in eukaryotic cells.[43] MGO is also present in a variety of foodstuffs such as honey and fermented products.[44,45] MGO is detoxified to lactate through a glutathione intermediate via the glyoxalase cycle, which is composed of lactoylglutathione lyase and hydroxyacylglutathione hydrolase (GLO1 and GLO2, respectively).[46] While elevations in MGO (10–100 μM) have been reported in diabetes, cancer, renal failure, and neurodegenerative diseases, the precise mechanisms underlying disease pathogenesis remain unknown.[42,46–49]

MGO covalently modifies guanine and adenine bases of DNA, RNA, and arginine, and lysine amino acid side chains of proteins (Figure 1).[3,50–52] These adducts are collectively referred to as advanced glycation end-products (AGEs). MGO activity leads to the formation of DNA–DNA cross-links.[53] MGO has also been shown to generate covalent DNA–protein cross-links. Early *in vitro* assays revealed MGO-mediated cross-linking of DNA polymerase 1 to 2′-deoxyguanosine.[3] More recently, MGO was shown to form covalent cross-links between 2′-deoxyguanosine and *N*-acetyl-lysine, as well as to cross-link histones to DNA in nucleosome core particles.[54,55] Additionally, SPRTN deficient cells and Ruijs–Aalfs patient lymphoblastoid cell lines with monogenic and biallelic mutations in SPRTN exhibit increased sensitivity to MGO.[56] Thus, mounting evidence suggests that MGO-derived DPCs may form in cells and play a role in human disease, warranting deeper exploration into this class of DNA lesions.

There is an unmet need to comprehensively profile and identify MGO-derived DPCs formed in cells. Earlier *in vitro* experiments have been limited to synthetic DNA duplexes which do not reflect normal DNA–protein interactions observed in cells. The purpose of the present study was to characterize DNA–protein cross-linking in human cells treated with MGO. Following treatment of human cells with MGO, biophysical DPC isolation assays were used to quantify DPC formation across different cell models. We utilized mass spectrometry-based proteomics to characterize proteins trapped to DNA upon MGO exposure. Our efforts

led to the identification of 265 proteins participating in cross-linking to DNA following MGO exposure, providing insight into potential DPCs that may be relevant in diseases linked to elevated MGO levels. Subsequent bioinformatic analyses revealed that these DPCs may influence chromatin architecture and telomere organization. *In vitro* experiments confirmed DPC formation by GAPDH and histone proteins H3.1 and H4 in the presence of MGO. Ultimately, this work provides initial information regarding DPC formation in living cells which serves as a starting point in studies aimed at understanding how MGO-induced DPCs may play a role in human disease.

RESULTS

DPC Formation in MGO-Treated Cells.

To investigate MGO-induced DPCs formation in human cells, we initially employed human embryonic kidney cells (HEK293T) as our cell model. To assess MGO toxicity in cells, HEK293T cells were treated with 50 μM–10 mM MGO for 2, 4, or 24 h, and their viability was assessed using the almarBlue assay. Treatment with MGO led to a dose-dependent decrease in cell viability (Figure 2A). Treatment with 10 mM MGO for 2, 4, and 24 h reduced cell viability to 75 ± 20%, 35 ± 18%, and 0.4 ± 1%, respectively. MGO induces oxidative stress, autophagy, and cell death.[57] To limit excessive cell death caused by MGO, we selected the 2 h MGO treatment window prior to DPC quantitation or isolation. Similar studies which generated cellular DPCs via treatment with cross-linking agents have also reported using 1–3 h long treatment times.[12,58–60]

To quantify the amounts of DPCs generated upon MGO treatment, we took advantage of the K-SDS assay.[61] In the K-SDS assay, samples denatured with sodium dodecyl sulfate (SDS) are treated with KCl, leading to precipitation of cellular proteins and any protein-bound DNA, while free DNA stays in solution. Following multiple rounds of protein precipitation and washing, any free DNA is removed, and DNA that coprecipitated with proteins is quantified to reveal the global DPC levels. The results are expressed as percent of cross-linked DNA of the total DNA input.[61] As shown in Figure 2B, DPC levels rose from 1.0% in untreated DNA to 2.2% in cells treated with 1 mM MGO and further to 8.8% in cells treated with 5 mM MGO. Additionally, we found that DPC levels in HEK293T cells as measured by the K-SDS assay modestly rose from 1.3% to 1.6% and 1.9% percent input upon treatment with physiologically relevant levels of MGO (10 μM and 100 μM, respectively). At lower MGO doses, MGO is efficiently metabolized leading to fewer cross-links which cannot be detected by the K-SDS assay due to its limited sensitivity. The presence of DPCs in untreated cells can be attributed to endogenous processes that trap proteins on DNA including enzymatic interactions during DNA unwinding, repair, replication, and recombination.[35,62,63]

We next assessed whether the loss of glyoxalase activity in cells may contribute to elevated levels of DPCs by preventing detoxification of MGO. We obtained HEK293T cells deficient in GLO1, one of the principal enzymes responsible for detoxifying MGO.[64–69] MGO treatment of GLO1-deficient cells led to a 2.4-fold increase in DPC formation as measured by the K-SDS assay (Figure 2C). These results indicate that GLO1-dependent detoxification pathways are important for protecting cells from DPC formation in the presence of MGO.

To determine whether MGO-dependent DPCs are recognized for proteolytic processing by SPRTN metalloprotease, we utilized $Sprtn^{F/-}$ mouse embryonic fibroblasts (MEF) cells with an intact floxed allele which exhibit reduced expression of SPRTN, a critical gene required for DPC proteolysis (Figure S1).[38,70] SPRTN is important for proteolytic processing of DPC lesions. Reduced SPRTN gene expression resulted in an elevated levels of DPCs in MEF cells exposed to 2.5 and 5 mM MGO (Figure 2D). These data indicate that DPCs generated by MGO can be recognized and cleaved by SPRTN metalloprotease.

To isolate proteins covalently linked to DNA in MGO-treated cells, we employed a modified phenol:chloroform extraction. This extraction enables isolation of DPCs via phase partitioning as they localize on the interface between aqueous and the organic solvent layer.[12,24,71] HT1080 cells were treated with 0.5, 1, 2.5, and 5 mM MGO, and the resulting DPCs were isolated using the modified phenol:chloroform method. The samples were normalized by total DNA content, separated by SDS-PAGE, and visualized via total protein staining (Figure 2E). MGO treatment produced observable protein bands, indicating dose-dependent DPC formation. These results corroborated the K-SDS results to confirm that MGO generates DPCs in human cells.

After detecting DPCs in MGO-treated human cells, we sought to determine the nature of amino acids and nucleosides participating in the formation of these cross-linked adducts and to quantify their levels in living cells. An authentic dG-MGO-Lys standard was synthesized in our laboratory and used to develop a quantitative HPLC-ESI-MS/MS method for its detection in cells. As shown in Figure 3A, dG-MGO-Lys was furnished in eight steps, by adapting a previously reported route.[54] We verified that the HPLC retention time and MS^2 fragmentation pattern of this standard were identical to the cross-linked product generated through the incubation of MGO dG and protected Lys, followed by Cbz deprotection (Figure S2), providing additional confidence in the structure of the cross-link. Next, HEK293T cells were treated with 5 mM MGO, and DPC containing genomic DNA was enzymatically digested with proteases and nucleases to form nucleoside-amino acid conjugates. dG-MGO-Lys adducts were subjected to offline reversed-phase HPLC fractionation and analyzed via HPLC–ESI^+-MS/MS. As shown in Figure 3B, MGO-treated cells produced a peak with the same retention time as the authentic dG-MGO-Lys standard. Based on external calibration curve, 5 mM MGO treatment led to 2.1 dG-MGO-Lys cross-links per million nucleotides while the same amount of DNA from vehicle-treated samples exhibited cross-link levels less than 0.18 cross-links per million nucleotides. These results indicate that dG-MGO-Lys cross-links form in living cells when MGO levels are elevated. By comparison, exogenous treatment with 2 mM diepoxybutane (DEB) was reported to form 6 cross-link adducts per million nucleotides.[6]

Identification of DPC Proteins by Mass Spectrometry-Based Proteomics.

Upon establishing that MGO exposure led to the formation of DPCs in human cell culture, we sought to identify the proteins participating in cross-linking. HT1080 cells were treated with 0 or 5 mM MGO for 2 h, and DPCs were isolated via modified phenol–chloroform extraction (Figure S3). A relatively high dose of MGO was chosen to maximize MGO-induced DPC formation for subsequent identification of cross-linked proteins in this “proof

of concept" study and is at a similar mM level used in other proteomics studies.[72–74] Following DPC extraction, samples were normalized by DNA content, and the proteins were analyzed via mass spectrometry-based proteomics. Proteomic analyses identified 265 DPC proteins that were enriched in the MGO treatment group ($p < 0.01$) Figure 4A and Table S1 contain a full listing of the proteins, including known DNA binders previously detected in other DNA–protein cross-linking studies including histones, GAPDH, PARP1, XRCC1, and TOP1.[6,24,59] Additionally, we verified that our proteomics results were consistent between biological replicates by correlating the label-free quantitation (LFQ) intensity values of identified proteins between all samples (Figure S4). We observed an R^2 correlation of 0.94 ± 0.02 for our MGO-treated samples ($N = 3$), indicating reproducible results for MGO-induced DPCs. Additionally, the R^2 correlation within the vehicle treatment group was moderate, 0.81 ± 0.07; whereas the R^2 correlation between MGO and vehicle groups was low, 0.47 ± 0.03, indicating that DPC enrichment via phenol:chloroform extraction and mass spectrometry analyses of the associated proteins are robust.

We next performed gene ontology (GO) analysis on this data set.[75,76] As shown in Figure 4B, a cellular compartment overrepresentation test with the DAVID database identified nuclear proteins associated with the nucleoplasm, nucleus, nucleolus, and chromatin to be significantly enriched. Of the proteins identified, 69.2% were classified as nuclear according to GO affiliation. These results are expected as nuclear proteins are in close proximity to DNA and are likely targets for MGO cross-linking. Although a significant number of proteins were classified by DAVID as ribosomal (10.5%) and membrane proteins (53.8%), many of these proteins can be found in multiple subcellular locations.[77] Indeed, further bioinformatics analysis of the enriched MGO-derived DPCs with STRING (Search Tool for the Retrieval of Interacting Genes/Proteins) revealed that the majority of these proteins possess multiple cellular compartment GO annotations (Figure S5).[78]

Subsequent bioinformatic analysis of the proteins participating in MGO-derived DPCs was performed using the DAVID biological process enrichment test (Figure 4C). Proteins involved in telomere organization and nucleosome assembly were found to be significantly enriched, suggesting that MGO-derived DPCs could affect nucleosome architecture. Interestingly, proteins participating in RNA-dependent processes were also enriched. Given that an RNAase digestion step was included in our phenol:chloroform extraction procedure to eliminate any RNA or RNA–protein conjugates, we hypothesize that these proteins also possess DNA binding activity. Additionally, previous studies of DPCs also found RNA-binding proteins enriched among the cross-linked targets.[6,24,59,79] Subsequent *k*-means clustering analysis of GO terms with the STRING bioinformatic database revealed five major clusters of MGO-derived DPCs with similar GO annotations which could be broadly classified into the following groupings: microtubule-based processes, rRNA processing, translation, nucleosome assembly, and RNA splicing (Figure S6). Additionally, previous studies of DPCs also found ribosomal proteins to be enriched among the cross-linked targets (Figure 4D and Table S2).[59] Collectively, these results indicate that MGO-induced DNA–protein cross-linking involves multiple classes of proteins and could disrupt multiple cellular pathways, potentially leading to toxicity.

To confirm our MS-based proteomics results, MGO-induced DPCs were subjected to dot blot analysis using commercial antibodies against specific DPC proteins. HT1080 cells were treated with 0.5, 1, 2.5, and 5 mM MGO for 2 h, and DPCs were extracted as described above. Samples were normalized based on DNA content and analyzed by dot blot using antibodies against PARP1, histone H3.1 XRCC1, TOP1, VINC, and GAPDH. These experiments revealed a dose-dependent increase of DPC protein abundance upon MGO exposure when normalized to dsDNA input (Figure 5B). As a negative control, we included the cytoplasmic protein GSTP1 which was not found detected among DPC proteins by MS-based proteomics. Blotting against isolated DPCs for GSTP1 did not display a dose-dependent increase in signal in DPC fraction upon MGO treatment.

Since DPC proteins have been reported to undergo ubiquitination and SUMOylation as part of proteolytic processing and repair and since ubiquitin and SUMO proteins were enriched in our proteomics results, DPCs extracted from MGO-treated cells were subjected to dot blot analysis probing for ubiquitin (UBB) and small ubiquitin-like modifier (SUMO), yielding a dose-dependent increase in signal (Figure S7). These results are consistent with a model that UBB and SUMO marks are being installed on MGO-generated DPCs, facilitating their repair. Collectively, our dot blot data are consistent with mass spectrometry-based proteomics results, confirming that PARP1, histone H3.1, XRCC1, TOP1, VINC, and GAPDH form DNA–protein cross-links in cells exposed to MGO.

In Vitro Confirmation of MGO-Induced DPC Formation.

As described above, our proteomics results have identified GAPDH and histones H3.1 and H4 among the proteins participating in MGO-mediated DPC formation (Figure 4). To confirm that these proteins participate in DNA–protein cross-linking upon exposure to MGO, we performed *in vitro* reactions using recombinant proteins and synthetic DNA strands and used gel shift assays to monitor DPC formation.

GAPDH is a moonlighting protein with many cellular functions including glycolysis and regulation of cell survival and apoptosis.[80] In previous studies, GAPDH has been reported to be susceptible to modification by MGO at its catalytic Cys residue and additional Arg and Lys sites, which can inhibit its enzymatic function.[81–85] Our mass spectrometry results confirmed that MGO covalently modifies GAPDH at multiple Lys and Arg residues (Table S3 and Figures S8–14). Importantly, GAPDH has been reported to bind telomeric DNA sequences with a K_d of 45 nM.[80] Given that bioinformatic analysis of the identified MGO DPCs found telomeric organization to be significantly enriched and that GAPDH is prone to MGO modification and can bind DNA, we sought to confirm that GAPDH is susceptible to cross-linking to DNA upon MGO treatment *in vitro*. To do so, recombinant GAPDH was incubated with a 3′ FAM-labeled single-stranded oligonucleotide featuring the telomeric sequence, $(TTAGGG)_3$, in the presence or absence of 10 mM MGO at pH 7.4. The reaction mixture was then subjected to SDS-PAGE to separate unmodified proteins from DPCs. Following separation, the DPCs were visualized via fluorescence imaging and protein staining as a higher-molecular-weight band. As shown in Figure 6A, a new band visualized by both fluorescent imaging and protein staining was observed upon MGO treatment of GAPDH and the FAM-labeled oligonucleotide, providing evidence for MGO-dependent

DPC formation. The molecular weight of this species was approximately 46 kDa, consistent with the theoretical size of the GAPDH–DNA conjugate. Furthermore, the cross-linking yield was dependent on MGO concentration and the duration of MGO treatment (Figure S15), consistent with DNA–GAPDH cross-linking in the presence of MGO. Gratifyingly, we found that the GAPDH DPCs formed under physiologically relevant MGO treatment concentrations of 100 μM.

To test the protein specificity for MGO-dependent DPC formation *in vitro*, we performed the same cross-linking experiment with the non-DNA-binding proteins which were not identified by proteomics, BSA and UBB. As shown in Figure S16, no new DPC bands were observed upon exposing these proteins to DNA and MGO, signifying that DNA–protein binding is likely an important factor in DPC formation by MGO. Additionally, we found that GAPDH which had been denatured by heating at 95 °C prior to cross-linking reaction did not form DPCs (Figure S17). Furthermore, incubation of GAPDH with a Lys reactive NHS-ester reagent to cap amine functionality prior to reaction with MGO and ss-telomeric DNA blocked cross-link formation (Figure S18). These results further suggest that DNA–protein interactions are needed for DPC formation via MGO and that MGO-induced cross-linking between GAPDH and DNA is mediated primarily through Lys side chains, although we cannot rule out the involvement of additional nucleophilic side chains such as Cys.[80,86] We also assessed the hydrolytic stability of MGO-induced GAPDH-DNA cross-links. Excess MGO was removed via molecular weight cutoff columns following a 3 h incubation of GAPDH with DNA and MGO, and the samples were subjected to further incubation at increasing time durations. As shown in Figure S19, the amounts of MGO-derived DPCs involving GAPDH diminished upon 16 h incubation at 37 °C, indicating modest stability of these adducts.

Histone proteins are bound to DNA and link cellular metabolism to gene expression and transcription through post-translational modifications.[87] In previous studies, histone proteins have been reported to be susceptible to MGO modification on their lysine-rich N-terminal tales.[55,88] Given that our proteomics results revealed histone proteins participation in DNA cross-linking, we sought to confirm that histone proteins H3.1 and H4 are susceptible to cross-linking to DNA upon MGO treatment *in vitro*. To do so, recombinant H3.1 and H4 were incubated with a ^{32}P-radiolabeled single-stranded oligonucleotide featuring the sequence, 5′-GTA AAA CGA CGG CCA GTG CCA AGC TTG CAT GCC TGC AGG TCG ACT CTA GAG GAT CCC CGG-3′, in the presence or absence of MGO at pH 7.4. The reaction mixture was then subjected to SDS-PAGE to separate unmodified DNA from DPCs. Following gel separation, the DPCs were visualized via phosphorimaging as high-molecular-weight bands. As shown in Figure 6B, new bands were observed in a dose-dependent manner upon MGO treatment of histone H3.1 and H4, indicating the cross-linking yield was dependent on MGO concentration. Furthermore, DPC bands reversed to free DNA following proteinase K treatment, providing additional evidence that these higher-molecular-weight bands are indeed DPCs. Collectively, these results indicate that histones are susceptible to cross-linking to DNA in the presence of MGO.

DISCUSSION

Identifying molecular mechanisms responsible for modulation of cellular phenotype by endogenous metabolites is critical for understanding the mechanisms by which metabolism contributes to overall health and disease.[89] Indeed, DNA–protein cross-links induced by endogenous compounds represent an important class of phenotype-altering event and many of the proteins participating in these cross-links remain unidentified due to challenges in DPC isolation and characterization. In this study, we investigated the formation of DNA–protein cross-links upon exposure of human cells in culture to electrophilic cellular metabolite MGO. MGO can participate in a variety of chemical reactions with biomolecules due to its electrophilic α-oxoaldehyde moiety.[90,91] MGO forms both protein and DNA adducts which can lead to inhibition of enzymatic activity, confirmational alterations, cell signaling events, depurination, formation of abasic sites, and induction of DNA protein cross-linking.[51,92–94]

Although previous studies reported the ability of MGO to form DNA–protein conjugates *in vitro*,[3,54,55] the relevance of these observations to living cells remained unknown, and the identities of other proteins participating in cross-linking had not been established. We took advantage of the K-SDS assay to quantify DPCs formation in MGO-treated human cells, while modified phenol:chloroform extraction procedure was used to isolate DPC for subsequent protein identification by mass spectrometry. This procedure has been used to identify proteins participating in DNA–protein cross-links.[6,24,59] MGO produced DPCs in human cells in a dose-dependent manner. We also showed that one possible chemical structure of MGO-derived DPC involves Lys protein residues and guanine in DNA based on comparison with an authentic analytical standard. However, it should be noted that other nucleophilic amino acid residues (Cys) and/or DNA bases may also be susceptible to cross-linking by MGO and should be explored in future work.[3] Additionally, analyzing MGO-derived DPCs with emerging DPC isolation techniques, like electro-elution of DPCs with agarose plugs,[95] will complement the phenol:chloroform extraction procedure utilized here as it may improve the isolation of high-molecular-weight DPCs that do not localize efficiently at the phenol–chloroform interface. Following DPC isolation from treated cells, proteins participating in DPC formation were identified by bottom-up proteomics. For this proof-of-concept work, we selected nonphysiological MGO concentrations (5 mM) to maximize our chances of detecting DPCs by liquimass spectrometry. Future work will be aimed at identifying MGO-derived DPCs at physiological MGO concentration and in disease models which have elevated MGO concentrations, such as various cancers and diabetes. We observed that MGO-treated human fibrosarcoma HT1080 cells contained DNA–protein cross-links that were heterogeneous in size and structure. The majority of these 265 cellular proteins that exhibited cross-linking characteristics are localized to the nucleus, nuclear chromosomes, telomere DNA regions, cellular membranes, and ribosomes. Additionally, dose-dependent cross-linking of a selected group of known DNA-binding proteins (histone H3.1, PARP1, XRCC1, GAPDH, VINC, and TOP1) to DNA in the presence of MGO was confirmed via dot blot analysis. The identified proteins are known to be involved in nucleosome assembly (e.g., histones, SMARCA5, NASP, START3), telomere organization (e.g., XRCC5, PARP1, Histones, RPA1), mRNA processing (e.g., helicases,

heterogeneous nuclear ribonucleoproteins, pre-mRNA processing factors), and DNA repair. DNA repair proteins over-represented in DPCs formed upon MGO exposure include BCCIP, FANCI, PDS5A, RECQL, RUVBL1, STUB1, SMARCA5, FEN1, MSH6, NONO, PARP1, RPA1, RPS3, TRIM28, UBR5, and SUMO. Currently, identifying the specific sites of amino acid–MGO–nucleobase cross-linking remains challenging given the heterogeneity of the DPC adducts and is a limitation of our current work. Future experiments will employ affinity enrichment methods to help determine specific cross-linking sites within cellular proteins.

Cellular repair mechanisms of DPCs is an active area of research.[96] Our results showed that reduced expression of the SPRTN gene which converts DPCs to less toxic peptide lesions led to elevated DPC levels upon 2.5 and 5 mM MGO treatment. Thus, it is likely that SPRTN plays a role in recognizing and removing MGO-derived DPCs, which is in line with previous reports finding SPRTN to be involved in repair of DPCs generated through formaldehyde.[30] Additionally, the observation that MGO treatment induces a dose-dependent increase in UBB and SUMO in isolated DPCs, coupled with finding UBB isoforms and SUMO to be enriched in our proteomic data set, suggests that ubiquitinylation and SUMOylation may be involved in repair of MGO-derived DPCs.[58] Based on previous studies, some of the possible repair mechanisms that could be involved in removing MGO cross-links include nucleotide excision repair (NER),[97,98] homologous recombination (HR),[99] and other proteolytic processes.[29] Future work will be needed to fully elucidate the predominant mechanisms underlying DPC repair and explore mutagenicity of this class of lesions.[41]

We observed that knockout of the GLO1 gene, which detoxifies MGO, significantly increased DPC levels upon MGO exposure. These results suggest that MGO-derived DPCs may be relevant adducts in aging and diseases associated with elevated MGO levels like diabetes, chronic renal disease, cancer, and Alzheimer's disease.[100–103]

To confirm our results for cell culture treatments, *in vitro* experiments utilizing recombinant GAPDH, histone H3.1, and histone H4 were conducted in order to characterize the cross-linking mechanisms and to establish the kinetics of cross-linking. It should be noted that MGO is known to covalently modify GAPDH, leading to enzymatic inhibition and alteration in isoelectric point.[81,82,84] In neural precursor cells (NPCs), it was found that MGO modification of GAPDH impacted Notch signaling which affected NPC homeostasis.[104] MGO-induced GAPDH–DNA cross-linking may play an additional role in the association between MGO and aging processes linked to telomeres; however, more detailed studies are needed to clarify this hypothesis.[50,105–108] MGO is also known to covalently modify histone proteins, leading to disruption of chromatin assembly and stability.[55,88] Breast cancer cells exhibit high levels of MGO-modified histone proteins.[55] These observations point toward a potential molecular mechanism linking metabolic perturbation and epigenetic deregulation in disease. Collectively, the reports of MGO protein modifications, coupled with our discovery that GAPDH and histone proteins H3.1 and H4 are targets for MGO-mediated DNA–protein cross-linking, point to the complexity of methylglyoxal biological activity and warrant continued investigation.

CONCLUSIONS

In conclusion, our study demonstrates that DNA–protein cross-links are readily formed in human fibrosarcoma HT1080 cells following exposure to mM levels of MGO. In these experiments, MGO exposure led to cross-linking of over 260 proteins to chromosomal DNA. These proteins were identified using mass spectrometry-based proteomics approaches, and the identities of selected cross-linked proteins were confirmed by immunoblotting. We verified that histone proteins and GAPDH cross-link to DNA oligonucleotides in the presence of MGO *in vitro*. Ongoing studies in our laboratory are using analytical standards to study the formation and repair of methylglyoxal-induced DPCs in the context of diabetes, neurological disorders, and cancer. Interrogating the functional ramifications of MGO-GAPDH DPCs and their mutagenetic potential, improving methods to identify the amino acids participating in DNA cross-linking, as well as conducting additional MGO DPC profiling experiments under physiological ranges of MGO concentrations are also underway. Ultimately, the work reported here provides a basis for studying MGO-derived DPCs to better understand mechanisms of MGO toxicity and MGO cell signaling events relevant in human disease.

Supplementary Material

Refer to Web version on PubMed Central for supplementary material.

ACKNOWLEDGMENTS

We would like to thank B. Carlson for his help with the figures for this manuscript.

Funding

This work was funded by a grant from NIEHS (ES023350, PIs: Tretyakova, N and Campbell) A.K.H. was partially supported by NIH Chemistry and Biology Interface Training grant T32 GM132029 and the University of Minnesota Doctoral Dissertation Fellowship. Contribution by J.J.G. was supported by R35GM137910 and R01DK133196. L.E. was supported by IRACDA program grant K12 GM119955–06 and by startup funds provided by the University of Kansas.

REFERENCES

(1). Merk O; Speit G Significance of formaldehyde-induced DNA-protein crosslinks for mutagenesis. Environ. Mol. Mutagen. 1998, 32 (3), 260–268. [PubMed: 9814441]

(2). Groehler AT; Kren S; Li Q; Robledo-Villafane M; Schmidt J; Garry M; Tretyakova N Oxidative cross-linking of proteins to DNA following ischemia-reperfusion injury. Free Radic. Biol. Med. 2018, 120, 89–101. [PubMed: 29540307]

(3). Murata-Kamiya N; Kamiya H Methylglyoxal, an endogenous aldehyde, crosslinks DNA polymerase and the substrate DNA. Nucleic Acids Res. 2001, 29 (16), 3433–3438. [PubMed: 11504881]

(4). Michaelson-Richie ED; Loeber RL; Codreanu SG; Ming X; Liebler DC; Campbell C; Tretyakova NY DNA-protein cross-linking by 1, 2, 3, 4-diepoxybutane. J. Proteome Res. 2010, 9 (9), 4356–4367. [PubMed: 20666492]

(5). Loeber R; Rajesh M; Fang Q; Pegg AE; Tretyakova N Cross-linking of the human DNA repair protein O^6-alkylguanine DNA alkyltransferase to DNA in the presence of 1, 2, 3, 4-diepoxybutane. Chem. Res. Toxicol. 2006, 19 (5), 645–654. [PubMed: 16696566]

(6). Gherezghiher TB; Ming X; Villalta PW; Campbell C; Tretyakova NY 1, 2, 3, 4-Diepoxybutane-induced DNA–protein cross-linking in human fibrosarcoma (HT1080) cells. J. Proteome Res. 2013, 12 (5), 2151–2164. [PubMed: 23506368]

(7). Barker S; Weinfeld M; Zheng J; Li L; Murray D Identification of mammalian proteins cross-linked to DNA by ionizing radiation. J. Biol. Chem. 2005, 280 (40), 33826–33838. [PubMed: 16093242]

(8). Barker S; Weinfeld M; Murray D DNA–protein crosslinks: Their induction, repair, and biological consequences. Mutat. Res. 2005, 589 (2), 111–135. [PubMed: 15795165]

(9). Zhitkovich A; Voitkun V; Kluz T; Costa M Utilization of DNA-protein cross-links as a biomarker of chromium exposure. Environ. Health Perspect. 1998, 106, 969–974. [PubMed: 9703480]

(10). Kloster M; Kostrhunova H; Zaludova R; Malina J; Kasparkova J; Brabec V; Farrell N Trifunctional dinuclear platinum complexes as DNA-protein cross-linking agents. Biochemistry 2004, 43 (24), 7776–7786. [PubMed: 15196020]

(11). Ewig RA; Kohn KW DNA damage and repair in mouse leukemia L1210 cells treated with nitrogen mustard, 1, 3-bis (2-chloroethyl)-1-nitrosourea, and other nitrosoureas. Cancer Res. 1977, 37, 2114–2122. [PubMed: 558823]

(12). Michaelson-Richie ED; Ming X; Codreanu SG; Loeber RL; Liebler DC; Campbell C; Tretyakova NY Mechlorethamine-induced DNA-protein cross-linking in human fibrosarcoma (HT1080) cells. J. Proteome Res. 2011, 10 (6), 2785–2796. [PubMed: 21486066]

(13). Baker JM; Parish JH; Curtis JPE DNA-DNA and DNA-protein crosslinking and repair in *Neurospora crassa* following exposure to nitrogen mustard. Mutat. Res., DNA Repair Rep. 1984, 132 (5–6), 171–179.

(14). Ewig RA; Kohn KW DNA-protein cross-linking and DNA interstrand cross-linking by haloethylnitrosoureas in L1210 cells. Cancer Res. 1978, 38 (10), 3197–3203. [PubMed: 150940]

(15). Wickramaratne S; Ji S; Mukherjee S; Su Y; Pence MG; Lior-Hoffmann L; Fu I; Broyde S; Guengerich FP; Distefano M; Schärer OD Bypass of DNA-protein cross-links conjugated to the 7-deazaguanine position of DNA by translesion synthesis polymerases. J. Biol. Chem. 2016, 291 (45), 23589–23603. [PubMed: 27621316]

(16). Oleinick NL; Chiu S; Ramakrishnan N; Xue LY The formation, identification, and significance of DNA-protein cross-links in mammalian cells. Br. J. Cancer Supplement 1987, 8, 135.

(17). Wickramaratne S; Boldry EJ; Buehler C; Wang Y-C; Distefano MD; Tretyakova NY Error-prone translesion synthesis past DNA-peptide cross-links conjugated to the major groove of DNA via C5 of thymidine. J. Biol. Chem. 2015, 290 (2), 775–787. [PubMed: 25391658]

(18). Tretyakova NY; Michaelson-Richie ED; Gherezghiher TB; Kurtz J; Ming X; Wickramaratne S; Campion M; Kanugula S; Pegg AE; Campbell C DNA-reactive protein monoepoxides induce cell death and mutagenesis in mammalian cells. Biochemistry 2013, 52 (18), 3171–3181. [PubMed: 23566219]

(19). Tretyakova NY; Ji S DNA-protein cross-links: Formation, structural identities, and biological outcomes. Acc. Chem. Res. 2015, 48 (6), 1631–1644. [PubMed: 26032357]

(20). Groehler Iv A; Degner A; Tretyakova NY Mass spectrometry-based tools to characterize DNA-protein cross-linking by *bis*-electrophiles. Basic Clin. Pharmacol. Toxicol. 2017, 121, 63–77. [PubMed: 28032943]

(21). Ruijs M; van Andel R; Oshima J; Madan K; Nieuwint AWM; Aalfs CM Atypical progeroid syndrome: An unknown helicase gene defect? Am. J. Med. Genet. Part A 2003, 116 (3), 295–299.

(22). Lessel D; Vaz B; Halder S; Lockhart PJ; Marinovic-Terzic I; Lopez-Mosqueda J; Philipp M; Sim JC; Smith KR; Oehler J; et al. Mutations in SPRTN cause early onset hepatocellular carcinoma, genomic instability and progeroid features. Nat. Genet. 2014, 46 (11), 1239–1244. [PubMed: 25261934]

(23). Lopez-Mosqueda J; Maddi K; Prgomet S; Kalayil S; Marinovic-Terzic I; Terzic J; Dikic I SPRTN is a mammalian DNA-binding metalloprotease that resolves DNA-protein crosslinks. Elife 2016, 5, No. e21491. [PubMed: 27852435]

(24). Groehler Iv A; Villalta PW; Campbell C; Tretyakova N Covalent DNA–protein cross-linking by phosphoramide mustard and nornitrogen mustard in human cells. Chem. Res. Toxicol. 2016, 29 (2), 190–202. [PubMed: 26692166]

(25). Ji S; Thomforde J; Rogers C; Fu I; Broyde S; Tretyakova NY Transcriptional bypass of DNA-protein and DNA-peptide conjugates by T7 RNA polymerase. ACS Chem. Biol. 2019, 14 (12), 2564–2575. [PubMed: 31573793]

(26). Thomforde J; Fu I; Rodriguez F; Pujari SS; Broyde S; Tretyakova N Translesion synthesis past 5-formylcytosine-mediated DNA-peptide cross-links by hPol η is dependent on the local DNA sequence. Biochemistry 2021, 60 (23), 1797–1807. [PubMed: 34080848]

(27). Yeo JE; Wickramaratne S; Khatwani S; Wang YC; Vervacke J; Distefano MD; Tretyakova NY Synthesis of site-specific DNA-protein conjugates and their effects on DNA replication. ACS Chem. Biol. 2014, 9 (8), 1860–1868. [PubMed: 24918113]

(28). Stingele J; Schwarz MS; Bloemeke N; Wolf PG; Jentsch S A DNA-dependent protease involved in DNA-protein crosslink repair. Cell 2014, 158 (2), 327–338. [PubMed: 24998930]

(29). Duxin JP; Dewar JM; Yardimci H; Walter JC Repair of a DNA-protein crosslink by replication-coupled proteolysis. Cell 2014, 159 (2), 346–357. [PubMed: 25303529]

(30). Stingele J; Bellelli R; Alte F; Hewitt G; Sarek G; Maslen SL; Tsutakawa SE; Borg A; Kjær S; Tainer JA; et al. Mechanism and regulation of DNA-protein crosslink repair by the DNA-dependent metalloprotease SPRTN. Mol. Cell 2016, 64 (4), 688–703. [PubMed: 27871365]

(31). Stingele J; Habermann B; Jentsch S DNA-protein crosslink repair: Proteases as DNA repair enzymes. Trends Biochem. Sci. 2015, 40 (2), 67–71. [PubMed: 25496645]

(32). Minko IG; Yamanaka K; Kozekov ID; Kozekova A; Indiani C; O'Donnell ME; Jiang Q; Goodman MF; Rizzo CJ; Lloyd RS Replication bypass of the acrolein-mediated deoxyguanine DNA-peptide cross-links by DNA polymerases of the DinB family. Chem. Res. Toxicol. 2008, 21 (10), 1983–1990. [PubMed: 18788757]

(33). Pujari SS; Tretyakova N Synthesis and polymerase bypass studies of DNA-peptide and DNA-protein conjugates. Methods Enzymol. 2021, 661, 363–405. [PubMed: 34776221]

(34). Naldiga S; Ji S; Thomforde J; Nicolae CM; Lee M; Zhang Z; Moldovan GL; Tretyakova NY; Basu AK Error-prone replication of a 5-formylcytosine-mediated DNA-peptide cross-link in human cells. J. Biol. Chem. 2019, 294 (27), 10619–10627. [PubMed: 31138652]

(35). Baker DJ; Wuenschell G; Xia L; Termini J; Bates SE; Riggs AD; O'Connor TR Nucleotide excision repair eliminates unique DNA-protein cross-links from mammalian cells. J. Biol. Chem. 2007, 282 (31), 22592–22604. [PubMed: 17507378]

(36). Chesner LN; Campbell C A quantitative PCR-based assay reveals that nucleotide excision repair plays a predominant role in the removal of DNA-protein crosslinks from plasmids transfected into mammalian cells. DNA Repair 2018, 62, 18–27. [PubMed: 29413806]

(37). Chesner LN; Essawy M; Warner C; Campbell C DNA-protein crosslinks are repaired via homologous recombination in mammalian mitochondria. DNA Repair 2021, 97, 103026. [PubMed: 33316746]

(38). Maskey RS; Flatten KS; Sieben CJ; Peterson KL; Baker DJ; Nam H-J; Kim MS; Smyrk TC; Kojima Y; Machida Y; et al. Spartan deficiency causes accumulation of Topoisomerase 1 cleavage complexes and tumorigenesis. Nucleic Acids Res. 2017, 45 (8), 4564–4576. [PubMed: 28199696]

(39). Larsen NB; Gao AO; Sparks JL; Gallina I; Wu RA; Mann M; Räschle M; Walter JC; Duxin JP Replication-coupled DNA-protein crosslink repair by SPRTN and the proteasome in xenopus egg extracts. Mol. Cell 2019, 73 (3), 574–588.e577. [PubMed: 30595436]

(40). Reardon JT; Cheng Y; Sancar A Repair of DNA-protein cross-links in mammalian cells. Cell Cycle 2006, 5 (13), 1366–1370. [PubMed: 16775425]

(41). Essawy M; Chesner L; Alshareef D; Ji S; Tretyakova N; Campbell C Ubiquitin signaling and the proteasome drive human DNA-protein crosslink repair. Nucleic Acids Res. 2023, 51 (22), 12174–12184. [PubMed: 37843153]

(42). Lai SWT; Lopez Gonzalez EJ; Zoukari T; Ki P; Shuck SC Methylglyoxal and its adducts: Induction, repair, and association with disease. Chem. Res. Toxicol. 2022, 35 (10), 1720–1746. [PubMed: 36197742]

(43). Rabbani N; Thornalley PJ Measurement of methylglyoxal by stable isotopic dilution analysis LC-MS/MS with corroborative prediction in physiological samples. Nat. Protoc. 2014, 9 (8), 1969–1979. [PubMed: 25058644]

(44). Nemet I; Varga-Defterdarović L; Turk Z Methylglyoxal in food and living organisms. Mol. Nutr. Food Res. 2006, 50 (12), 1105–1117. [PubMed: 17103372]

(45). Zheng J; Guo HY; Ou JY; Liu PZ; Huang CH; Wang MF; Simal-Gandara J; Battino M; Jafari SM; Zou L; et al. Benefits, deleterious effects and mitigation of methylglyoxal in foods: A critical review. Trends Food Sci. Technol. 2021, 107, 201–212.

(46). Thornalley PJ Pharmacology of methylglyoxal: Formation, modification of proteins and nucleic acids, and enzymatic detoxification-a role in pathogenesis and antiproliferative chemotherapy. Gen. Pharmacol. 1996, 27 (4), 565–573. [PubMed: 8853285]

(47). Kilhovd BK; Juutilainen A; Lehto S; Rönnemaa T; Torjesen PA; Hanssen KF; Laakso M Increased serum levels of methylglyoxal-derived hydroimidazolone-AGE are associated with increased cardiovascular disease mortality in nondiabetic women. Atherosclerosis 2009, 205 (2), 590–594. [PubMed: 19185865]

(48). Agalou S; Ahmed N; Babaei-Jadidi R; Dawnay A; Thornalley PJ Profound mishandling of protein glycation degradation products in uremia and dialysis. J. Am. Soc. Nephrol. 2005, 16 (5), 1471–1485. [PubMed: 15800128]

(49). Trujillo MN; Galligan JJ Reconsidering the role of protein glycation in disease. Nat. Chem. Biol. 2023, 19 (8), 922–927. [PubMed: 37430113]

(50). Thornalley PJ Protein and nucleotide damage by glyoxal and methylglyoxal in physiological systems-role in ageing and disease. Drug Metabol. Drug Interact. 2008, 23 (1–2), 125–150. [PubMed: 18533367]

(51). Frischmann M; Bidmon C; Angerer J; Pischetsrieder M Identification of DNA adducts of methylglyoxal. Chem. Res. Toxicol. 2005, 18 (10), 1586–1592. [PubMed: 16533023]

(52). Bidmon C; Frischmann M; Pischetsrieder M Analysis of DNA-bound advanced glycation end-products by LC and mass spectrometry. J. Chromatogr. B 2007, 855 (1), 51–58.

(53). Rahman A; Shahabuddin; Hadi SM Formation of strand breaks and interstrand cross-links in DNA by methylglyoxal. J. Biochem. Toxicol. 1990, 5 (3), 161–166. [PubMed: 2283666]

(54). Petrova KV; Millsap AD; Stec DF; Rizzo CJ Characterization of the deoxyguanosine–lysine cross-link of methylglyoxal. Chem. Res. Toxicol. 2014, 27 (6), 1019–1029. [PubMed: 24801980]

(55). Zheng Q; Omans ND; Leicher R; Osunsade A; Agustinus AS; Finkin-Groner E; D'Ambrosio H; Liu B; Chandarlapaty S; Liu S; Yael D Reversible histone glycation is associated with disease-related changes in chromatin architecture. Nat. Commun. 2019, 10 (1), 1289. [PubMed: 30894531]

(56). Vaz B; Popovic M; Newman JA; Fielden J; Aitkenhead H; Halder S; Singh AN; Vendrell I; Fischer R; Torrecilla I; et al. Metalloprotease SPRTN/DVC1 orchestrates replication-coupled DNA-protein crosslink repair. Mol. Cell 2016, 64 (4), 704–719. [PubMed: 27871366]

(57). Lee JH; Parveen A; Do MH; Kang MC; Yumnam S; Kim SY Molecular mechanisms of methylglyoxal-induced aortic endothelial dysfunction in human vascular endothelial cells. Cell Death Dis. 2020, 11 (5), 403. [PubMed: 32467587]

(58). Sun Y; Miller Jenkins LM; Su YP; Nitiss KC; Nitiss JL; Pommier Y A conserved SUMO pathway repairs topoisomerase DNA-protein cross-links by engaging ubiquitin-mediated proteasomal degradation. Sci. Adv. 2020, 6 (46), No. eaba6290. [PubMed: 33188014]

(59). Ming X; Groehler Iv A; Michaelson-Richie ED; Villalta PW; Campbell C; Tretyakova NY Mass spectrometry based proteomics study of cisplatin-induced DNA-protein cross-linking in human fibrosarcoma (HT1080) cells. Chem. Res. Toxicol. 2017, 30 (4), 980–995. [PubMed: 28282121]

(60). Loeber RL; Michaelson-Richie ED; Codreanu SG; Liebler DC; Campbell CR; Tretyakova NY Proteomic analysis of DNA-protein cross-linking by antitumor nitrogen mustards. Chem. Res. Toxicol. 2009, 22 (6), 1151–1162. [PubMed: 19480393]

(61). Zhitkovich A; Costa M A simple, sensitive assay to detect DNA-protein crosslinks in intact cells and in vivo. Carcinogenesis 1992, 13 (8), 1485–1489. [PubMed: 1499101]

(62). Connelly JC; Leach DR Repair of DNA covalently linked to protein. Mol. Cell 2004, 13 (3), 307–316. [PubMed: 14967139]

(63). Verdine GL; Norman DP Covalent trapping of protein-DNA complexes. Annu. Rev. Biochem. 2003, 72, 337–366. [PubMed: 14527324]

(64). Lee J-Y; Song J; Kwon K; Jang S; Kim C; Baek K; Kim J; Park C Human DJ-1 and its homologs are novel glyoxalases. Hum. Mol. Genet. 2012, 21 (14), 3215–3225. [PubMed: 22523093]

(65). Morgenstern J; Fleming T; Schumacher D; Eckstein V; Freichel M; Herzig S; Nawroth P Loss of glyoxalase 1 induces compensatory mechanism to achieve dicarbonyl detoxification in mammalian Schwann cells. J. Biol. Chem. 2017, 292 (8), 3224–3238. [PubMed: 27956549]

(66). Schumacher D; Morgenstern J; Oguchi Y; Volk N; Kopf S; Groener JB; Nawroth PP; Fleming T; Freichel M Compensatory mechanisms for methylglyoxal detoxification in experimental & clinical diabetes. Mol. Metab. 2018, 18, 143–152. [PubMed: 30287091]

(67). Vander Jagt DL; Hunsaker LA Methylglyoxal metabolism and diabetic complications: Roles of aldose reductase, glyoxalase-I, betaine aldehyde dehydrogenase and 2-oxoaldehyde dehydrogenase. Chem.-Biol. Interact 2003, 143, 341–351. [PubMed: 12604221]

(68). Vander Jagt DL; Robinson B; Taylor K; Hunsaker L Reduction of trioses by NADPH-dependent aldo-keto reductases. Aldose reductase, methylglyoxal, and diabetic complications. J. Biol. Chem. 1992, 267 (7), 4364–4369. [PubMed: 1537826]

(69). Gaffney DO; Jennings EQ; Anderson CC; Marentette JO; Shi T; Schou Oxvig AM; Streeter MD; Johannsen M; Spiegel DA; Chapman E Non-enzymatic lysine lactoylation of glycolytic enzymes. *Cell* Chem. Biol. 2020, 27 (2), 206–213.e6.

(70). Maskey RS; Kim MS; Baker DJ; Childs B; Malureanu LA; Jeganathan KB; Machida Y; Van Deursen JM; Machida YJ Spartan deficiency causes genomic instability and progeroid phenotypes. Nat. Commun. 2014, 5 (1), 5744. [PubMed: 25501849]

(71). Sambrook J; Russell DW Purification of nucleic acids by extraction with phenol: Chloroform. CSH Protoc. 2006, 2006 (1), pdb. prot4455. [PubMed: 22485786]

(72). Bollong MJ; Lee G; Coukos JS; Yun H; Zambaldo C; Chang JW; Chin EN; Ahmad I; Chatterjee AK; Lairson LL; et al. A metabolite-derived protein modification integrates glycolysis with KEAP1-NRF2 signalling. Nature 2018, 562 (7728), 600–604. [PubMed: 30323285]

(73). Chen X; Liu Y; Kong L; Wen Z; Wang W; Wang C Quantitative chemoproteomic profiling of protein cross-links induced by methylglyoxal. *ACS* Chem. Biol. 2022, 17 (8), 2010–2017.

(74). Sibbersen C; Schou Oxvig AM; Bisgaard Olesen S; Nielsen CB; Galligan JJ; Jørgensen KA; Palmfeldt J; Johannsen M Profiling of methylglyoxal blood metabolism and advanced glycation end-product proteome using a chemical probe. ACS Chem. Biol. 2018, 13 (12), 3294–3305. [PubMed: 30508371]

(75). Huang DW; Sherman BT; Lempicki RA Systematic and integrative analysis of large gene lists using DAVID bioinformatics resources. Nat. Protoc. 2009, 4 (1), 44–57. [PubMed: 19131956]

(76). Huang DW; Sherman BT; Lempicki RA Bioinformatics enrichment tools: Paths toward the comprehensive functional analysis of large gene lists. Nucleic Acids Res. 2009, 37 (1), 1–13. [PubMed: 19033363]

(77). Mélèse T; Xue Z The nucleolus: An organelle formed by the act of building a ribosome. Curr. Opin. Cell Biol. 1995, 7 (3), 319–324. [PubMed: 7662360]

(78). Szklarczyk D; Franceschini A; Wyder S; Forslund K; Heller D; Huerta-Cepas J; Simonovic M; Roth A; Santos A; Tsafou KP; et al. STRING v10: Protein–protein interaction networks, integrated over the tree of life. Nucleic Acids Res. 2015, 43 (D1), D447–D452. [PubMed: 25352553]

(79). Stützer A; Welp LM; Raabe M; Sachsenberg T; Kappert C; Wulf A; Lau AM; David SS; Chernev A; Kramer K; et al. Analysis of protein-DNA interactions in chromatin by UV induced cross-linking and mass spectrometry. Nat. Commun. 2020, 11 (1), 5250. [PubMed: 33067435]

(80). Demarse NA; Ponnusamy S; Spicer EK; Apohan E; Baatz JE; Ogretmen B; Davies C Direct binding of glyceraldehyde 3-phosphate dehydrogenase to telomeric DNA protects telomeres against chemotherapy-induced rapid degradation. J. Mol. Biol. 2009, 394 (4), 789–803. [PubMed: 19800890]

(81). Irshad Z; Xue M; Ashour A; Larkin JR; Thornalley PJ; Rabbani N Activation of the unfolded protein response in high glucose treated endothelial cells is mediated by methylglyoxal. Sci. Rep. 2019, 9 (1), 7889. [PubMed: 31133647]

(82). Coukos JS; Lee CW; Pillai KS; Liu KJ; Moellering RE Widespread, reversible cysteine modification by methylglyoxal regulates metabolic enzyme function. ACS Chem. Biol. 2023, 18 (1), 91–101. [PubMed: 36562291]

(83). Ray M; Basu N; Ray S Inactivation of glyceraldehyde-3-phosphate dehydrogenase of human malignant cells by methylglyoxal. Mol. Cell. Biochem. 1997, 177, 21–26. [PubMed: 9450641]

(84). Lee HJ; Howell SK; Sanford RJ; Beisswenger PJ Methylglyoxal can modify GAPDH activity and structure. Ann. N. Y. Acad. Sci. 2005, 1043, 135–145. [PubMed: 16037232]

(85). Donnellan L; Young C; Simpson BS; Acland M; Dhillon VS; Costabile M; Fenech M; Hoffmann P; Deo P Proteomic analysis of methylglyoxal modifications reveals susceptibility of glycolytic enzymes to dicarbonyl stress. Int. J. Mol. Sci. 2022, 23 (7), 3689. [PubMed: 35409048]

(86). White MR; Khan MM; Deredge D; Ross CR; Quintyn R; Zucconi BE; Wysocki VH; Wintrode PL; Wilson GM; Garcin ED A dimer interface mutation in glyceraldehyde-3-phosphate dehydrogenase regulates its binding to AU-rich RNA. J. Biol. Chem. 2015, 290 (3), 1770–1785. [PubMed: 25451934]

(87). Galdieri L; Vancura A Acetyl-CoA carboxylase regulates global histone acetylation. J. Biol. Chem. 2012, 287 (28), 23865–23876. [PubMed: 22580297]

(88). Galligan JJ; Wepy JA; Streeter MD; Kingsley PJ; Mitchener MM; Wauchope OR; Beavers WN; Rose KL; Wang T; Spiegel DA; et al. Methylglyoxal-derived posttranslational arginine modifications are abundant histone marks. Proc. Natl. Acad. Sci. U. S. A. 2018, 115 (37), 9228–9233. [PubMed: 30150385]

(89). Long MJ; Huang K-T; Aye Y The not so identical twins: (dis) similarities between reactive electrophile and oxidant sensing and signaling. Chem. Soc. Rev. 2021, 50 (22), 12269–12291. [PubMed: 34779447]

(90). Schalkwijk C; Stehouwer C Methylglyoxal, a highly reactive dicarbonyl compound, in diabetes, its vascular complications, and other age-related diseases. Physiol. Rev. 2020, 100 (1), 407–461. [PubMed: 31539311]

(91). Kold-Christensen R; Johannsen M Methylglyoxal metabolism and aging-related disease: Moving from correlation toward causation. Trends Endocrinol. Metab. 2020, 31 (2), 81–92. [PubMed: 31757593]

(92). Vaca CE; Fang J-L; Conradi M; Hou S-M Development of a ^{32}P-postlabelling method for the analysis of 2'-deoxyguanosine-3′-monophosphate and DNA adducts of methylglyoxal. Carcinogenesis 1994, 15 (9), 1887–1894. [PubMed: 7923582]

(93). Oya T; Hattori N; Mizuno Y; Miyata S; Maeda S; Osawa T; Uchida K Methylglyoxal modification of protein: Chemical and immunochemical characterization of methylglyoxal-arginine adducts. J. Biol. Chem. 1999, 274 (26), 18492–18502. [PubMed: 10373458]

(94). Bento CF; Marques F; Fernandes R; Pereira P Methylglyoxal alters the function and stability of critical components of the protein quality control. PLoS One 2010, 5 (9), No. e13007. [PubMed: 20885985]

(95). Weickert P; Li HY; Götz MJ; Dürauer S; Yaneva D; Zhao S; Cordes J; Acampora AC; Forne I; Imhof A; et al. SPRTN patient variants cause global-genome DNA-protein crosslink repair defects. Nat. Commun. 2023, 14 (1), 352. [PubMed: 36681662]

(96). Stingele J; Bellelli R; Boulton SJ Mechanisms of DNA-protein crosslink repair. Nat. Rev. Mol. Cell Biol. 2017, 18 (9), 563–573. [PubMed: 28655905]

(97). Tamae D; Lim P; Wuenschell GE; Termini J Mutagenesis and repair induced by the DNA advanced glycation end product N2–1-(carboxyethyl)-2'-deoxyguanosine in human cells. Biochemistry 2011, 50 (12), 2321–2329. [PubMed: 21355561]

(98). Nakano T; Morishita S; Katafuchi A; Matsubara M; Horikawa Y; Terato H; Salem AM; Izumi S; Pack SP; Makino K; et al. Nucleotide excision repair and homologous recombination systems commit differentially to the repair of DNA-protein crosslinks. Mol. Cell 2007, 28 (1), 147–158. [PubMed: 17936711]

(99). Nakano T; Katafuchi A; Matsubara M; Terato H; Tsuboi T; Masuda T; Tatsumoto T; Pack SP; Makino K; Croteau DL; et al. Homologous recombination but not nucleotide excision repair plays a pivotal role in tolerance of DNA-protein cross-links in mammalian cells. J. Biol. Chem. 2009, 284 (40), 27065–27076. [PubMed: 19674975]

(100). Rabbani N; Thornalley PJ Dicarbonyl stress in cell and tissue dysfunction contributing to ageing and disease. Biochem. Biophys. Res. Commun. 2015, 458 (2), 221–226. [PubMed: 25666945]

(101). Rabbani N; Thornalley PJ Advanced glycation end products in the pathogenesis of chronic kidney disease. Kidney Int. 2018, 93 (4), 803–813. [PubMed: 29477239]

(102). Rabbani N; Xue M; Thornalley PJ Activity, regulation, copy number and function in the glyoxalase system. Biochem. Soc. Trans. 2014, 42 (2), 419–424. [PubMed: 24646254]

(103). Distler MG; Palmer AA Role of Glyoxalase 1 (Glo1) and methylglyoxal (MG) in behavior: Recent advances and mechanistic insights. Front. Genet. 2012, 3, 36946.

(104). Rodrigues DC; Harvey EM; Suraj R; Erickson SL; Mohammad L; Ren M; Liu H; He G; Kaplan DR; Ellis J; et al. Methylglyoxal couples metabolic and translational control of Notch signalling in mammalian neural stem cells. Nat. Commun. 2020, 11 (1), 2018. [PubMed: 32332750]

(105). Maessen DE; Stehouwer CD; Schalkwijk CG The role of methylglyoxal and the glyoxalase system in diabetes and other age-related diseases. Clin. Sci. 2015, 128 (12), 839–861.

(106). Aubert G; Lansdorp PM Telomeres and aging. Physiol. Rev. 2008, 88 (2), 557–579. [PubMed: 18391173]

(107). Loecken EM; Guengerich FP Reactions of glyceraldehyde 3-phosphate dehydrogenase sulfhydryl groups with bis-electrophiles produce DNA-protein cross-links but not mutations. Chem. Res. Toxicol. 2008, 21 (2), 453–458. [PubMed: 18163542]

(108). Savreux-Lenglet G; Depauw S; David-Cordonnier M-H Protein recognition in drug-induced DNA alkylation: When the moonlight protein GAPDH meets S23906–1/DNA minor groove adducts. Int. J. Mol. Sci. 2015, 16 (11), 26555–26581. [PubMed: 26556350]

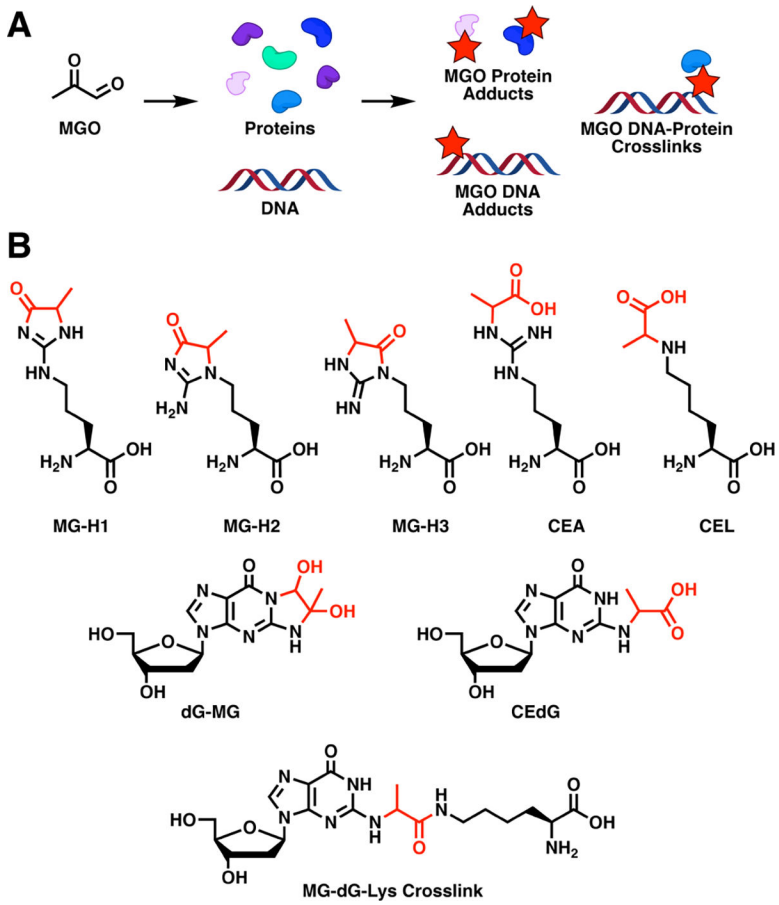

Figure 1.

Reaction of methylglyoxal with a variety of biomolecules. (A) Schematic of MGO forming covalent adducts to proteins and DNA or generating DNA–protein cross-links. (B) Chemical structures of various MGO adducts with amino acid side chains, DNA bases, and proposed DNA–protein cross-links. Shown here are methylglyoxal-derived hydroimidazolone 1–3 (MG-H1–3), *Nε*-carboxyethylarginine (CEA), *Nε*-carboxyethyllysine (CEL), 6,7-dihydroxy-3-(−4-hydroxy-5-(hydroxymethyl)tetrahydrofuran-2-yl)-6-methyl-3,5,6,7-tetrahydro-9*H*-imidazo[1,2-*a*]purin-9-one (dG-MG), N2-(1-carboxtethyl)guanine (CEdG), and N6-(9-(−4-hydroxy-5-(hydroxymethyl)tetrahydrofuran-2-yl)-6-oxo-6,9-dihydro-1*H*-purin-2-yl)alanyl)-L-lysine (MG-dG-Lys cross-link).

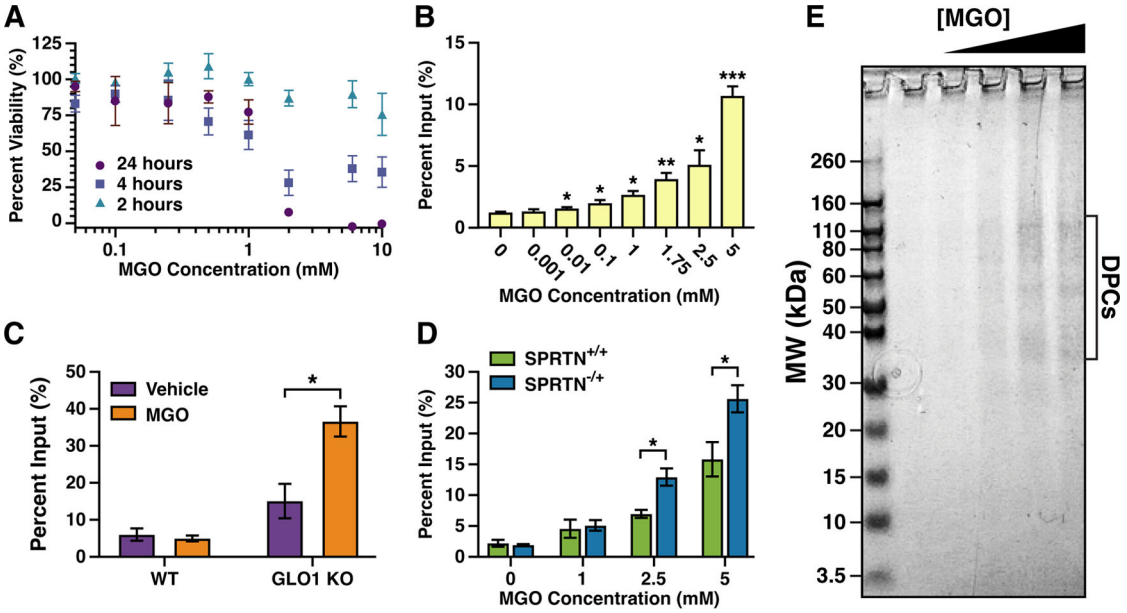

Figure 2.

Generation of DPCs in cellular models by MGO treatment. (A) MGO reduces HEK293T cell viability as a function of time and concentration. HEK293T cells were treated with MGO at multiple time points and concentrations. Viability was determined through an alamarBlue assay. Data is represented as mean ± SEM from four replicates and normalized to vehicle control. (B) MGO treatment generates DPCs in HEK293T cells. HEK293T cells were treated with 0, 0.001, 0.01, 0.1, 1.0, 1.75, 2.5, or 5 mM MGO for 2 h and were processed by the K-SDS assay to quantify DPC levels. Data are represented as mean ± SEM from three replicates and normalized to DNA input and were analyzed via a one-way ANOVA and an unpaired *t* test (**p* < 0.05). (C) Knockout of GLO1 leads to increased levels of DPC formation following MGO treatment. HEK293T cells with or without GLO1 were treated with 0 or 1 mM MGO for 2 h and were processed by the K-SDS assay to quantify DPC levels. Data are represented as mean ± SEM from three replicates and normalized to DNA input and were analyzed via a one-way ANOVA and an unpaired *t* test (**p* < 0.05). (D) Reduced SPRTN expression leads to increased levels of DPC formation following MGO treatment. MEF cells with or without SPRTN deficiency were treated with 0, 1, 2.5, or 5 mM MGO for 2 h and then processed by the K-SDS assay to quantify DPC levels. Data are represented as mean ± SEM from three replicates and normalized to DNA input and were analyzed via a one-way ANOVA and an unpaired *t* test (**p* < 0.05). (E) Visualization of MGO-induced DPCs isolated via phenol-chloroform extraction. HT1080 cells were treated with 0, 0.5, 1, 2.5, or 5 mM MGO for 2 h and were processed by the phenol–chloroform extraction to isolate DPCs. Isolated DPCs were resolved by 4–12% SDS–PAGE and visualized by the Simply Blue protein stain.

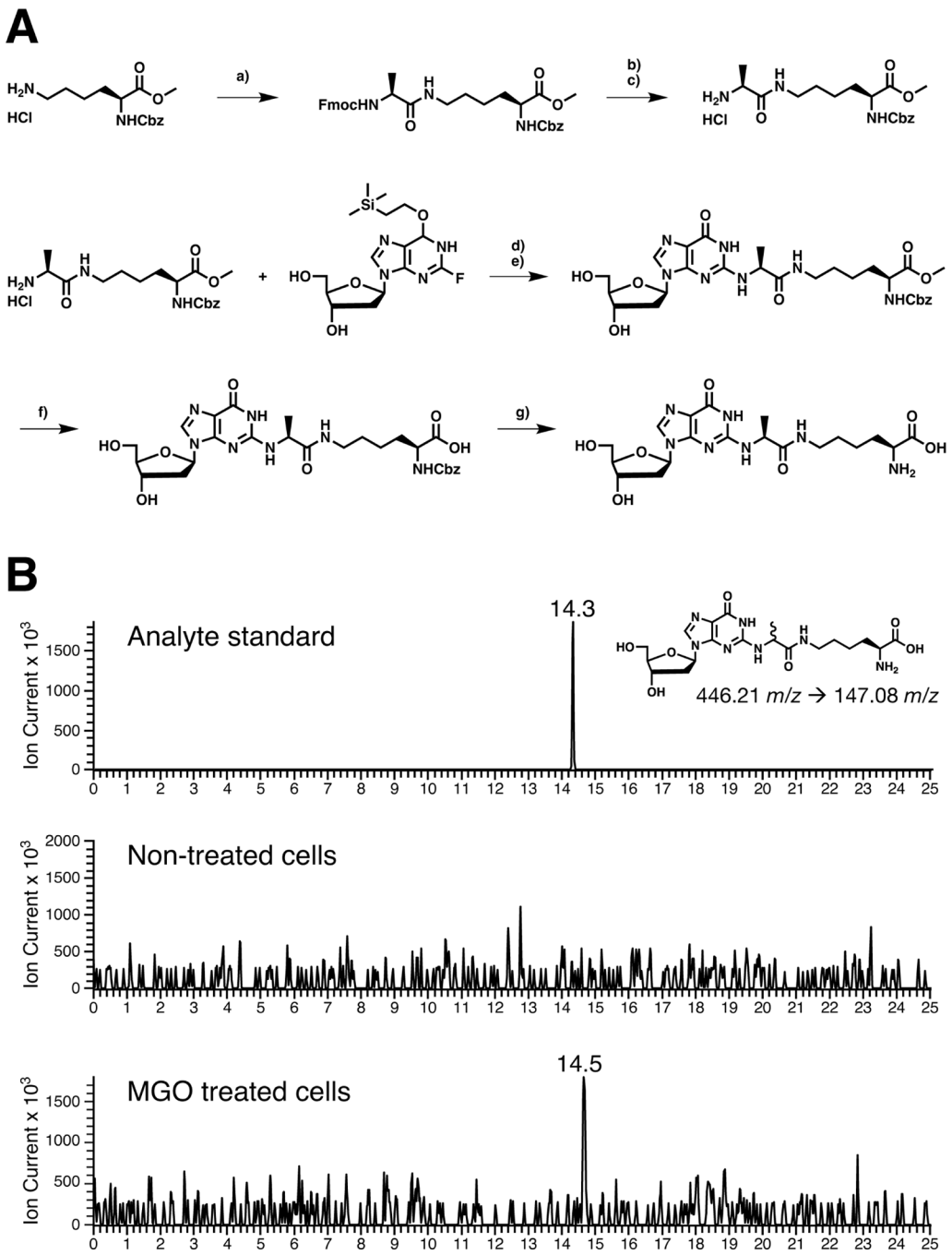

Figure 3.

Synthesis of dG-MGO-Lys cross-link standard and detection of dG-MGO-Lys cross-link in human cells upon MGO treatment. (A) Overview of synthetic route to dG-MGO-Lys cross-link standard: (a) FmocAla, HCTU, DIPEA, DMF; (b) 20% piperidine, DMF; (c) 4 M HCl, dioxane, 52% (3 steps); (d) DIPEA, DMSO; (e) TBAF, THF, 37% (2 steps); (f) LiOH, H_2O, THF, 41%; (g) H_2, Pd/C, MeOH, 65%. (B) HEK293T cells were treated with 0 or 5 mM MGO for 2 h and processed by DNAzol and DNA precipitation to isolate DPCs. DPCs were digested with protease K and nucleases, subjected to offline RP-HPLC purification,

and analyzed via HPLC–ESI-MS/MS using selected reaction monitoring (m/z 468.2 $m/z \rightarrow$ 147.1).

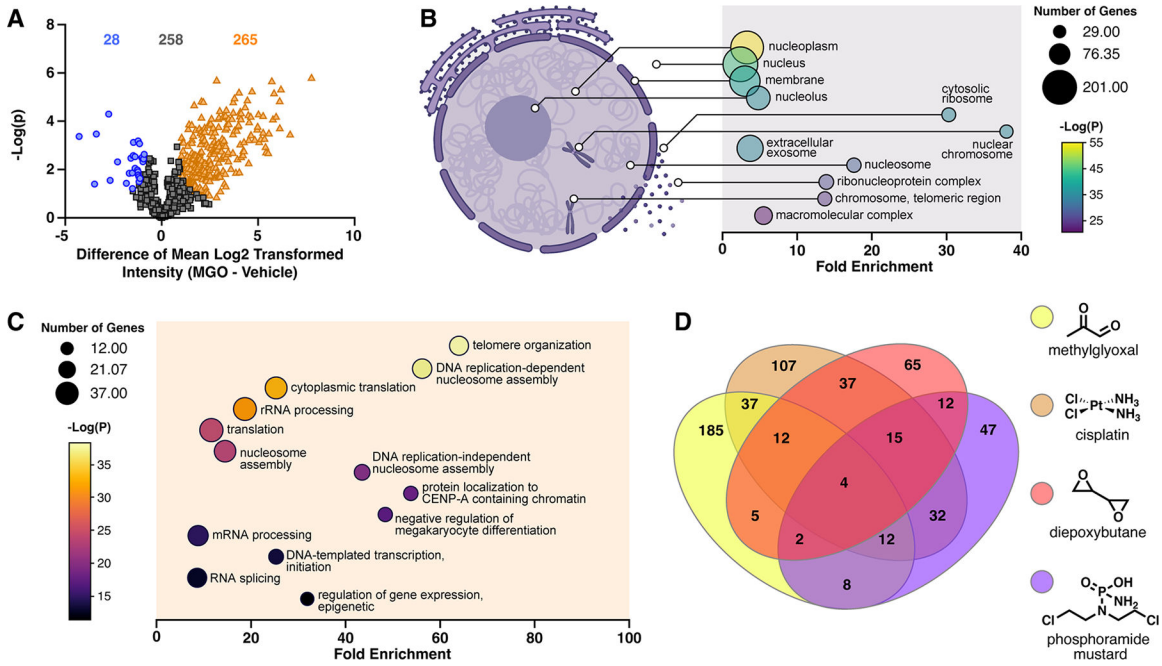

Figure 4.

Mass spectrometry-based proteomics results for MGO-derived DPCs. (A) Volcano plot of proteins identified as potential MGO DPCs. HT1080 cells were treated with 0 or 5 mM MGO for 2 h and then subjected to modified phenol-chloroform extraction to isolate DPCs. DPCs were identified via LC–MS/MS and statistically analyzed for enrichment at an FDR of 0.01 and a minimal coefficient of variation (S0) of 0.5. Proteins highlighted in orange were significantly enriched in the MGO-treated samples, while those in blue were more abundant in vehicle treatment group. Data are representative of 3 biological replicates from each treatment condition. (B) Cellular compartment analysis of DPCs enriched by MGO treatment. Analysis was performed with the DAVID overrepresentation test, and results are shown as a multivariable plot with the Benjamini–Hochberg adjusted *p*-value, number of genes, and fold enrichment displayed for each enriched GO cellular compartment term. (C) Biological process analysis of DPCs enriched by MGO treatment. Analysis was performed with the DAVID overrepresentation test, and results are shown as a multivariable plot with the Benjamini–Hochberg adjusted *p*-value, number of genes, and fold enrichment displayed for each enriched GO biological process term. (D) Depiction of DPCs identified in HT1080 cells upon exposure to diepoxybutane,[6] cisplatin,[59] phosphoramide mustard,[24] and MGO (this work). Venn diagram shows the number of overlapped identified proteins between each condition. Color is representative of cross-linker treatment.

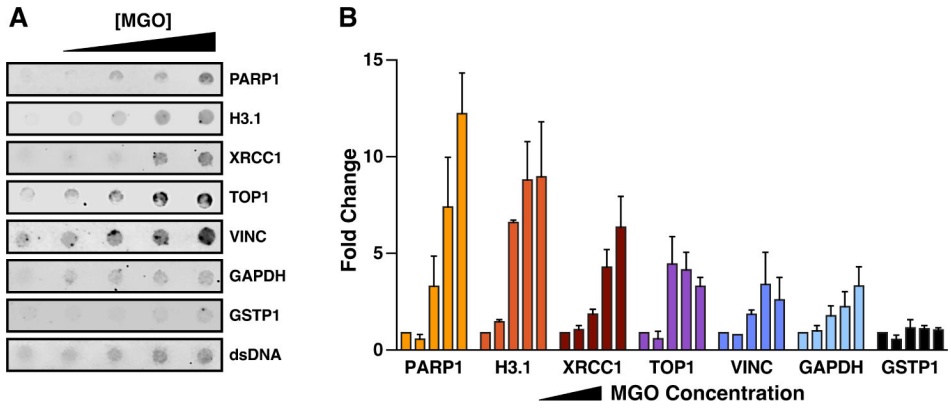

Figure 5.

Dot blot analysis of MGO-induced DPCs. (A) Representative dot blots of DPCs isolated via phenol–chloroform extraction from HT1080 cells treated with 0, 0.5, 1, 2.5, or 5 mM MGO for 2 h. Samples were normalized for DNA content, immobilized on nitrocellulose membranes, and probed with primary antibodies specific for PARP1, histone H3.1 XRCC1, TOP1, VINC, GAPDH, GSTP1, and dsDNA. (B) Fold change in measured dot blot fluorescence intensity for indicted protein signal normalized to input dsDNA for 0, 0.5, 1, 2.5, or 5 mM MGO treatments, shown left to right for each protein, respectively. Data are represented as mean ± SEM from at least two biological replicates.

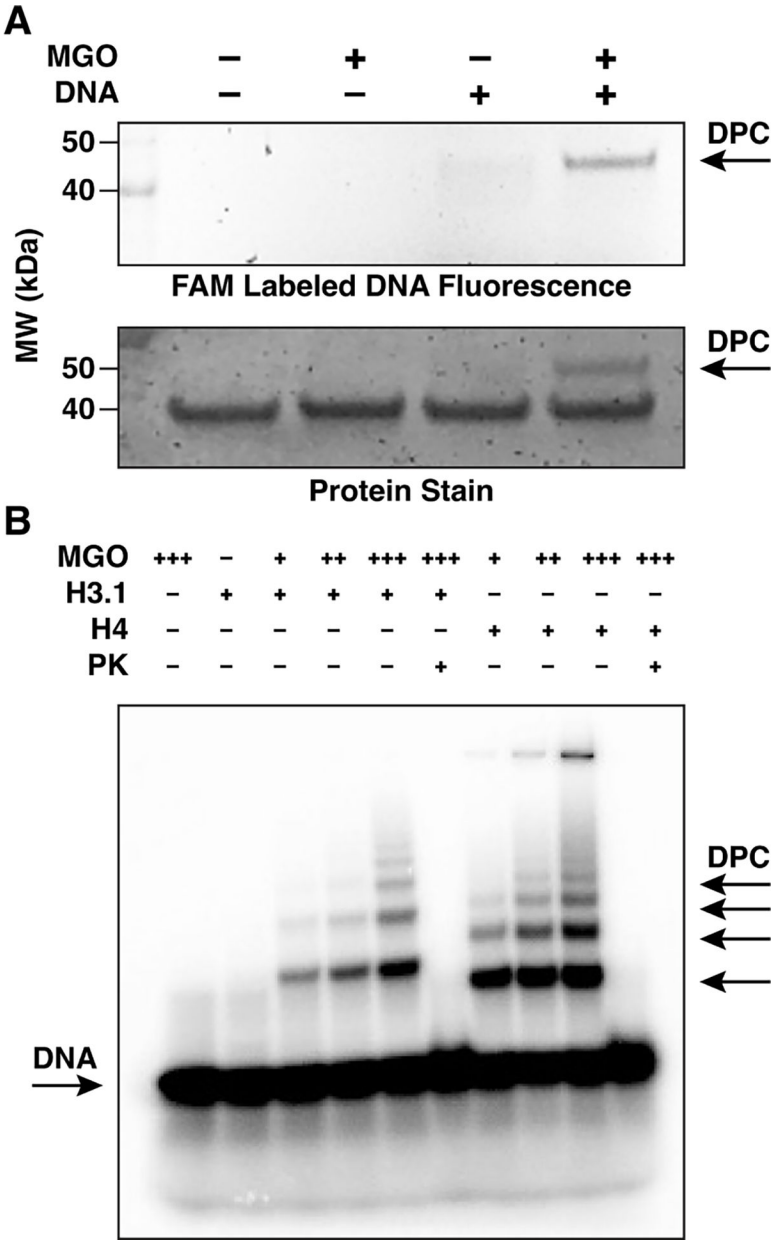

Figure 6.

In vitro confirmation of MGO-induced DPC formation in the presence of MGO. A) Representative gel of GAPDH (1 μg) incubated with or without FAM-labeled ss-telomeric DNA $(TTAGGG)_3$ (25 μM) in the presence or absence of MGO (10 mM) in 25 μL of PBS (pH 7.4) at 37 °C for 1 h; top: FAM fluorescence; bottom: silver stain. B) Representative gel images of histones H3.1 and H4 (6.67 μM) incubated with 60-mer ^{32}P-radiolabeled single-stranded oligonucleotide (0.83 μM) in the absence or presence of MGO (21, 42, and 83 μM) in PBS (pH 7.4) at 37 °C for 16 h (total reaction volume: 30 μL). For proteinase K (PK) treatment, PK was added into the reaction mixtures following MGO cross-linking

and the mixtures were further incubated at 37 °C for 24 h prior to SDS-PAGE analysis. Radioactivity within the gels was imaged via phosphor imaging.